Observation of Heteronuclear Atomic Efimov Resonances

G. Barontini,[1] C. Weber,[2] F. Rabatti,[1] J. Catani,[1,3] G. Thalhammer,[1] M. Inguscio,[1,3] and F. Minardi[1,3]

[1]*LENS, European Laboratory for Non-Linear Spectroscopy and Dipartimento di Fisica, Università di Firenze, via Nello Carrara 1, I-50019 Sesto Fiorentino, Firenze, Italy*

[2]*Institut für Angewandte Physik, Universität Bonn, Wegelerstraße 8, D-53115 Bonn, Germany*

[3]*CNR-INFM, via G. Sansone 1, I-50019 Sesto Fiorentino, Firenze, Italy*

(Received 27 January 2009; published 20 July 2009)

Building on the recent experimental observation with ultracold atoms, we report the first experimental evidence of Efimov physics in a heteronuclear system. A mixture of ^{41}K and ^{87}Rb atoms was cooled to few hundred nanokelvins and stored in an optical dipole trap. Exploiting a broad interspecies Feshbach resonance, the losses due to three-body collisions were studied as a function of the interspecies scattering length. We observe an enhancement of the three-body collisions for three distinct values of the interspecies scattering lengths, both positive and negative, where no Feshbach resonances are expected. We attribute the two features at negative scattering length to the existence of two kinds of Efimov trimers, KKRb and KRbRb.

DOI: 10.1103/PhysRevLett.103.043201 PACS numbers: 34.50.−s, 36.40.−c, 21.45.−v, 67.85.−d

Sun-earth-moon, the helium atom, the proton: at all length scales, three-body systems are ubiquitous in physics, yet they challenge our understanding in many ways. Their complexity conspicuously exceeds the two-body counterparts. A peculiar class of three-body systems defying our intuition arises when the constituents feature resonant pairwise interactions, such that the scattering length is much larger than the effective range of the pair potential. In a few seminal papers, Efimov advanced our understanding of such three-body systems and demonstrated the existence of a large number of weakly bound three-body states, thereafter known as the *Efimov effect* [1,2]. What makes Efimov states truly remarkable is their *universality*, i.e., the fact that their main properties are independent from the details of the pair potential, be it the strong interaction between two nucleons or the van der Waals force between two neutral atoms.

For over 35 years, the Efimov effect has sparked intense theoretical research [3], while eluding experimental observation. The first evidence of Efimov states was reached in a pioneering experiment with ultracold ^{133}Cs atoms, exploiting a Feshbach resonance to adjust the scattering length [4]. However, the Efimov effect is not limited to the case of three identical particles, but applies to a broader range of systems. For example, there is an ongoing debate about the prospects of observing Efimov states in nuclear physics [5], the original context studied by Efimov. In nuclear physics the strong long range Coulomb interactions confines the Efimov effect to triads where at least two constituents are neutral. Halo nuclei like ^{6}He, ^{11}Li, ^{14}Be, ^{20}C, which are composed of a smaller core nucleus plus two loosely bound neutrons, have been identified as possible examples of Efimov physics [6]. Therefore extending the study of Efimov physics from homonuclear systems, for which new experimental evidences recently emerged [7–10], to systems composed of distinguishable particles with different masses [11,12] provides a more complete understanding of the Efimov physics, where many results are known only for homonuclear systems [3].

In this Letter, we report the first experimental evidence of Efimov physics with particles of different masses, i.e., Efimov resonances in the three-body collisions of a mixture of ultracold ^{41}K and ^{87}Rb atoms. Our experiment demonstrates that two resonantly interacting pairs are sufficient to grant the existence of Efimov states [3] and, due to the mentioned universal properties, suggests that they could be observed also in other asymmetric triads, like the halo nuclei.

In ultracold atomic gases, direct association of bound Efimov states has never been achieved but their existence is revealed by measuring the atomic losses, since it bears a dramatic impact in the three-body recombination (3BR)

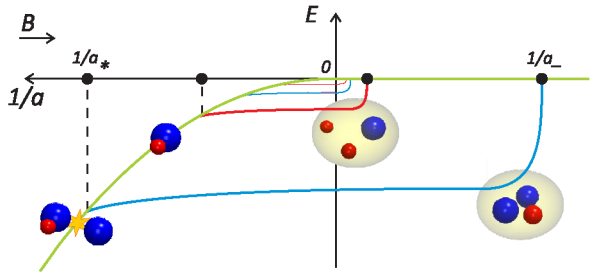

FIG. 1 (color online). Pictorial energy diagram of Efimov states for the double-species mixture of K and Rb, around an interspecies Feshbach resonance where the K-Rb scattering length diverges ($1/a = 0$). The Efimov resonances appear: (i) at the atom-dimer threshold for positive scattering lengths a_*; (ii) at the three-atoms threshold for negative scattering lengths a_-. Two distinct kinds of Efimov trimer are possible, KKRb (red or dark gray line) and KRbRb (blue or gray). The green or light gray line shows the dissociation threshold of the Efimov states.

collisions [3,4], and by the enhancement of atom-dimer collisions [9,13]. The energy of Efimov states depends on the resonant scattering length, as depicted in Fig. 1. For a certain negative value of the scattering length $a = a_-$, the binding energy of an Efimov state vanishes; i.e., the energy of the trimer coincides with the energy of three free atoms. At this scattering length a_-, the 3BR collisions are resonantly enhanced [4]. For positive values of the scattering length, the 3BR rate displays an oscillatory behavior with broad maxima and minima [14,15]. In addition, at a scattering length value a_*, the Efimov trimers energy hits the atom-dimer threshold: here, a resonant enhancement occurs for the atom-dimer collisions, both elastic and inelastic [13]. In the limit of infinite $|a|$, the above features repeat for each state of the Efimov spectrum as the scattering length is multiplied by integer powers of a scaling factor, usually denoted with e^{π/s_0}, which does not depend on the details of the interaction potential. This scenario holds only in the "universal" regime, i.e., when the scattering length is much larger than the van der Waals length ℓ_{vdW} [16], that is the relevant range of the interatomic potential. In our case, $\ell_{\mathrm{vdW}} = 72a_0$ for the KRb interaction potential [17], with a_0 denoting the Bohr radius. On the other hand, while the values of the resonant scattering lengths a_* and a_- depend on the details of the atomic potential and are so far unpredictable, theoretical predictions are available for their ratios a_*/a_-, in the case of identical particles [3,18]. For the heteronuclear case the scaling laws of 3BR rates have been derived [19], but explicit predictions for the 3BR loss rate coefficients, the atom-dimer elastic cross section and inelastic rate, and the ratio a_*/a_-, are still lacking.

With the mixture of ^{41}K and ^{87}Rb, we have four distinct three-body loss channels, two homonuclear and two heteronuclear, the latter being enhanced by the proximity of an interspecies Feshbach resonance [20]. Correspondingly, there exist two Efimov series, namely, in the KKRb and KRbRb channels shown in Fig. 1, whose relative location is so far unpredictable. The two series have widely different scaling factors $e^{\pi/s_0} = 3.51 \times 10^5$ for KKRb and 131 for KRbRb [12]. The first Efimov resonance is expected to appear in the range $\ell_{\mathrm{vdW}} < |a_-| < \ell_{\mathrm{vdW}} e^{\pi/s_0}$, i.e., $|a_-|/a_0 < 9.4 \times 10^3$ for the KRbRb channel, and $|a_-|/a_0 < 2.5 \times 10^7$ for KKRb. As explained below, at finite temperatures the unitarity limit of the 3BR rate narrows the range of useful scattering lengths. Thus, *a priori* the detection of an Efimov resonance is much more likely in KRbRb than in KKRb.

We now briefly describe our experimental procedure. We prepare the ultracold atomic mixture by sympathetic cooling, first in a magnetic trap and then in a crossed dipole trap ($\lambda = 1064$ nm), far off-resonant with respect to both K and Rb atomic transitions [20]. We cool the mixture to temperatures as low as 300 nK, while trapping it in a harmonic potential ($\omega_{\mathrm{Rb}} \simeq 2\pi \times 70$ Hz, $\omega_{\mathrm{K}} = \omega_{\mathrm{Rb}}\sqrt{m_{\mathrm{Rb}}/m_{\mathrm{K}}}$). Both species are prepared in the $|F = 1, m_F = 1\rangle$ states, featuring a broad interspecies Feshbach resonance at 38.4 G [21], which allows us to adjust the interspecies scattering length a. Since the $|1, 1\rangle$ state is the absolute ground state, inelastic two-body collisions are suppressed. The final stage of evaporation is performed at a uniform magnetic field (Feshbach field) of 76 G, that is subsequently ramped to the final value in 20 ms. At this point, we typically have 10^5 Rb and 5×10^4 K atoms at 400 nK (peak densities equal to 2×10^{12} cm^{-3} and 1×10^{12} cm^{-3}, respectively). We then hold the Feshbach field constant while the atom number decays due to 3BR losses [22]. Then, we switch off the trap and separately image the expanding clouds of remnant K and Rb atoms. An example of atom decay during the hold time is shown in Fig. 2. We record the atom number as we scan the interspecies scattering length varying the Feshbach field. For the best signal-to-noise ratio, we use the total atom number $N(t_h) = N_{\mathrm{K}}(t_h) + N_{\mathrm{Rb}}(t_h)$ after a fixed hold time t_h as our main observable. This quantity is the least affected by the fluctuations of the K-Rb population balance, boosted by the sympathetic cooling. The atom numbers of individual species, N_{K} and N_{Rb}, are used to ascertain the dominant channel of three-body losses at the resonance peaks. Since our losses are due to 3BR collisions, $N(t_h)$ yields the same information as the 3BR rate, as far as the positions of the Efimov resonances are concerned. It also provides immediate indications on the relative widths of the Efimov resonances.

On the side of negative scattering length, i.e., for magnetic fields above 38.4 G, we observe two peaks of three-body losses above a smooth increase with the scattering length (see Fig. 3). The broadest peak, strong and visible up to temperatures of approximately 0.8 μK, is centered at a magnetic field of 57.7(5) G. The second peak, weaker and not visible above 0.3 μK, lies at 38.8(1) G. Conversion of these magnetic field values into scattering length is done with the aid of the numerical results of the collisional model of the K-Rb potential [17], based on extensive studies of Feshbach spectroscopy [23,24] combined with

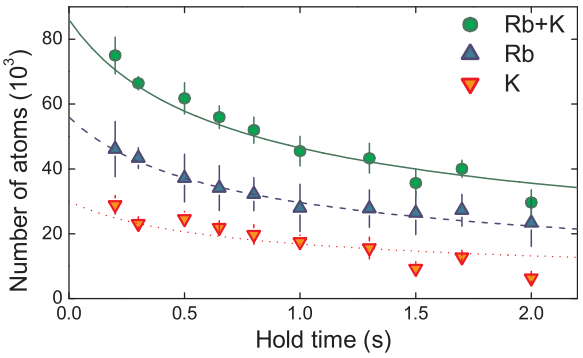

FIG. 2 (color online). Decay of the number of atoms trapped in our crossed dipole trap at $B = 56.8$ G. At this magnetic field only collisions in KRbRb channel are relevant: the collision rate α_{KRbRb} equals $1.9(7) \times 10^{-23}$ cm^6/s. The lines show the results of our numerical model including only KRbRb 3BR collisions. Hereafter, the error bars represent 1 standard deviation.

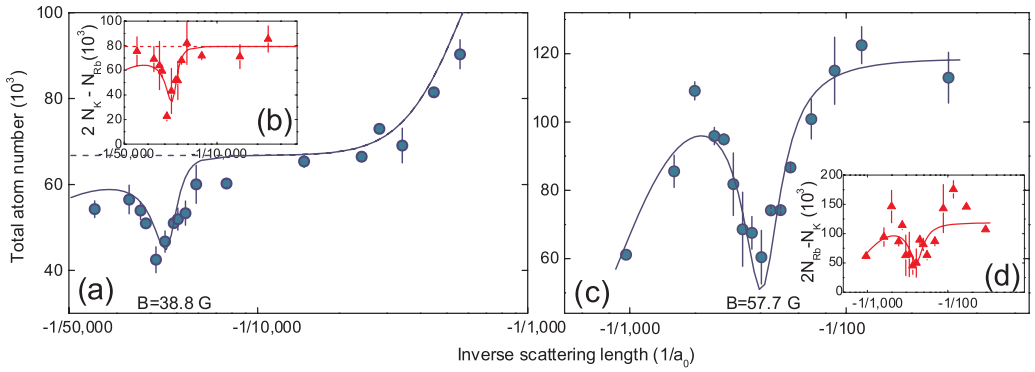

FIG. 3 (color online). Peaks of inelastic atomic losses at 38.8 G (a),(b) and 57.7 G (c),(d), signaling the Efimov resonances at negative scattering lengths in the KKRb and KRbRb channel, respectively. We show the total number of atoms $N_K + N_{Rb}$ remaining in the optical trap after a fixed hold time at the given scattering length (a),(c). The hold times and temperatures are: 100 ms and 0.3 μK (a), 500 ms and 0.4 μK (c). The solid lines refer to the numerical results of our model. The dashed lines (a),(b) show the result of numerical integration taking into account only KRbRb collisions. In the insets (b) and (d) we plot the linear combinations $2N_K - N_{Rb}$ and $2N_{Rb} - N_K$, respectively, supporting the channel assignment of the Efimov peaks (see text).

our recent spectroscopy measurements of the weakly bound molecular state [21].

To make sure that the peaks are genuine interspecies 3-body features, we have taken the following steps. First, we verified that both loss peaks are absent if we prepare samples with only a single species. Second, according to the collisional model, at the corresponding magnetic field values no sufficiently broad Feshbach resonances occur, even considering molecular levels with angular momentum $\ell = 1, 2$ [25]. We also checked that the frequency offset between the crossed trap beams is sufficiently far detuned with respect to any bound state, in order to avoid Raman transition to molecular levels. Finally, on the stronger peak the time evolution of the individual species atom number shows (Fig. 2) that the ratio of lost Rb to K atoms is 1.7(3), which unambiguously proves this peak is due to 3BR and it is dominated by the KRbRb channel. For different magnetic fields, however, the signal-to-noise of the atomic decay is insufficient to distinguish between the different 3BR channels. Thus, for the weaker peak at 38.8 G, we analyze the individual species atom number at fixed hold time. From our data set we calculate the linear combination $2N_K - N_{Rb}$, that is expected to be constant for KRbRb collisions and to display a negative peak for KKRb collisions. Such a peak is indeed observed [Fig. 3(b)] and, since the experimental data for $2N_K - N_{Rb}$ nicely agree with our numerical results, we assign it to the KKRb channel. For comparison, we also plot the combination $2N_{Rb} - N_K$ for the peak at 57.7 G [Fig. 3(d)].

To derive the 3BR rates, we model the loss process by a set of differential rate equations. We start from the local rate equations for the atom densities n_K and n_{Rb}, i.e., $\dot{n}_K = -2\alpha_{KKRb} n_K^2 n_{Rb} - \alpha_{KRbRb} n_K n_{Rb}^2$ and $\dot{n}_{Rb} = -\alpha_{KKRb} n_K^2 n_{Rb} - 2\alpha_{KRbRb} n_K n_{Rb}^2$ where α_{KKRb} and α_{KRbRb} denote the event collision rates in the KKRb and KRbRb 3BR channels. By integration upon coordinates, we obtain the rate equations for the atom numbers N_K, N_{Rb}. In addition, we also consider recombination heating and evaporation [22], taking into account the displacement between the two species due to the differential gravity sag. The set of (four) differential equations, for atom number and total energy of each species, is numerically integrated. In analogy with the case of identical particles, the 3BR rate α_{KRbRb} is taken to be [19]

$$\alpha_{KRbRb} = C \frac{\sinh 2\eta}{\sin^2[s_0(\delta)\log(a/a_-)] + \sinh^2\eta} \frac{\hbar a_\delta^4}{\mu_\delta}$$

with $\delta = m_K/m_{Rb}$, $a_\delta = a\sqrt[4]{\delta(\delta+2)}/\sqrt{\delta+1}$, and $\mu_\delta = m_K/\sqrt{\delta(\delta+2)}$. Likewise, we assume the equivalent expression for α_{KKRb}, with independent C, a_-, η parameters. The mass-dependent scaling parameter $s_0(\delta)$ equals 0.644 for KRbRb and 0.246 for KKRb. The positions, widths, and multiplicative factors (a_-, η, C) are adjusted to match the numerical results of the above rate equations with the measured number of atoms.

For the weaker peak at 38.8 G, it is crucial to introduce the unitary limit, i.e., a maximum value of 3BR rate that we take to be of the same order of magnitude as that of homonuclear systems [26]. In practice, *for each channel* we replace the appropriate α with an effective $\alpha_{eff} = \alpha_{max}\alpha/(\alpha_{max} + \alpha)$ approximately equal to the minimum between α and $\alpha_{max} \sim 20\pi^2\hbar/(\mu_\delta k^4)$, with the latter depending on temperature through $(\hbar k)^2 = 2\mu_\delta k_B T$. The output of the numerical integration, shown in Fig. 3 agrees nicely with data, once we adjust the parameters to the following values: $a_- = -246(14)a_0$, $\eta = 0.12(1)$ and $C = 34(16) \times 10^2$ for α_{KRbRb} and $a_- = -22(^{+4}_{-6}) \times 10^3 a_0$, $\eta = 0.017(10)$ and $C = 6(4) \times 10^{-4}$ for α_{KKRb}. The uncertainties on the positions reflect the estimated uncertainty on the magnetic field values.

We find that the KRbRb channel dominates 3BR collisions at nearly all magnetic fields, with the exception of a narrow region next to the Feshbach resonance where we

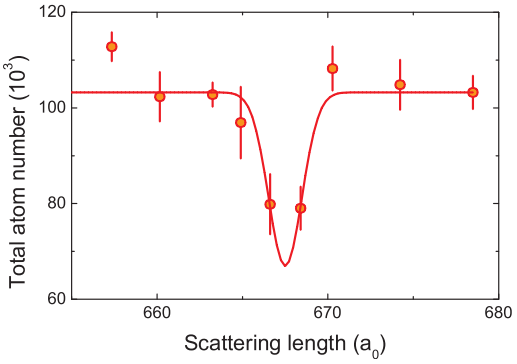

FIG. 4 (color online). Peak of enhanced inelastic atom losses at positive scattering lengths, corresponding to a possible atom-dimer resonance at 4.2 G. We show the total number of atoms $N_K + N_{Rb}$ remaining in the optical trap after a fixed hold time of 500 ms at the given scattering length. These data were taken at a temperature of 400 nK, each point averages on 2 to 5 experimental runs. The solid line is a Gaussian fit.

detect the Efimov peak of the KKRb channel [see dashed lines in Fig. 3(a)]. It is important to note that this peak is observable because, at these magnetic fields, the dominant KRbRb channel is limited by unitarity, while the much weaker KKRb channel is not.

For positive scattering length, the three-body inelastic collision rate is expected to display an oscillatory behavior with no sharp peaks [14,15]. However, we did not observe any clear oscillation in the range 0–38.4 G corresponding to $a > 650a_0$, only a peak of atomic losses at $B = 4.25(0.10)$ G, corresponding to $a = 667(1)a_0$. Loss peaks at positive values of the scattering length have been recently reported in ^{39}K and attributed to resonantly enhanced secondary collisions between atoms and dimers created in 3BR processes [10]. For values of the scattering length $a = a_*$ resonances occur in the atom-dimer scattering [9], similar to Feshbach resonances. In analogy with [10], the narrow peak of losses at 4.2 G, shown in Fig. 4, could be due to an atom-dimer resonance. With the same arguments as above, we can exclude inelastic two-body collisions to be the cause of this peak. Since for this peak we lose more Rb than K atoms, the atom-dimer resonance should belong to the KRbRb channel. Further experimental investigations are in order, along with the theoretical predictions extending the results on the atom-dimer scattering to heteronuclear systems [18] at finite temperature.

In summary, we have observed three distinct peaks of the inelastic collision rate of the mixture ^{41}K^{87}Rb near an interspecies Feshbach resonance. Two of these peaks represent Efimov resonances, of both the KKRb and KRbRb channel, occurring at values of the interspecies scattering length a such that the binding energy of Efimov trimers vanishes. Our data represent the first unambiguous observation of Efimov physics in systems composed of distinguishable particles with different masses and the first experimental demonstration that two resonant interactions are sufficient for Efimov physics to take place. These findings have a direct impact on the search of Efimov physics in a broad domain of physical systems, e.g., nuclear physics. We foresee that in the future more Efimov physics will emerge especially with very asymmetric systems composed of one particle which is much lighter than the other two [12]: for such systems, the scaling factor approaches 1 and several consecutive Efimov states could be detected. Among Bose-Bose mixtures, very promising combinations are LiYbYb ($e^{\pi/s_0} \simeq 4.5$ [12]), LiCsCs ($e^{\pi/s_0} \simeq 5.5$), as well as LiRbRb ($e^{\pi/s_0} \simeq 7.9$) where an interspecies Feshbach resonance has already been observed [27].

We acknowledge fruitful discussions with M. Zaccanti, P. G. Bizzeti, J. P. D'Incao, M. Jona-Lasinio, G. Modugno, and G. Poggi. Funding was provided by CNR (EuroQUAM DQS, QUDIPMOL), EU (STREP CHIMONO, NAMEQUAM) and Ente CRF.

[1] V. Efimov, Phys. Lett. B **33**, 563 (1970).
[2] V. Efimov, Yad. Fiz. **12**, 1080 (1970) [Sov. J. Nucl. Phys. **12**, 589 (1971)].
[3] E. Braaten and H.-W. Hammer, Phys. Rep. **428**, 259 (2006).
[4] T. Krämer *et al.*, Nature (London) **440**, 315 (2006).
[5] I. Mazumdar, A. R. P. Rau, and V. S. Bhasin, Phys. Rev. Lett. **97**, 062503 (2006).
[6] A. S. Jensen, K. Riisager, D. V. Fedorov, and E. Garrido, Rev. Mod. Phys. **76**, 215 (2004).
[7] T. B. Ottenstein *et al.*, Phys. Rev. Lett. **101**, 203202 (2008).
[8] J. H. Huckans *et al.*, Phys. Rev. Lett. **102**, 165302 (2009).
[9] S. Knoop *et al.*, Nature Phys. **5**, 227 (2009).
[10] M. Zaccanti *et al.*, Nature Phys. (to be published).
[11] R. D. Amado and J. V. Noble, Phys. Rev. D **5**, 1992 (1972).
[12] V. Efimov, Nucl. Phys. **A210**, 157 (1973).
[13] E. Nielsen, H. Suno, and B. D. Esry, Phys. Rev. A **66**, 012705 (2002).
[14] E. Nielsen and J. H. Macek, Phys. Rev. Lett. **83**, 1566 (1999).
[15] B. D. Esry, C. H. Greene, and J. P. Burke, Phys. Rev. Lett. **83**, 1751 (1999).
[16] E. L. Bolda, E. Tiesinga, and P. S. Julienne, Phys. Rev. A **66**, 013403 (2002).
[17] A. Simoni *et al.*, Phys. Rev. A **77**, 052705 (2008).
[18] K. Helfrich and H.-W. Hammer (private communication).
[19] J. P. D'Incao and B. D. Esry, Phys. Rev. A **73**, 030702(R) (2006).
[20] G. Thalhammer *et al.*, Phys. Rev. Lett. **100**, 210402 (2008).
[21] C. Weber *et al.*, Phys. Rev. A **78**, 061601(R) (2008).
[22] T. Weber *et al.*, Phys. Rev. Lett. **91**, 123201 (2003).
[23] F. Ferlaino *et al.*, Phys. Rev. A **73**, 040702(R) (2006).
[24] C. Klempt *et al.*, Phys. Rev. A **76**, 020701(R) (2007).
[25] G. Thalhammer *et al.*, New J. Phys. **11**, 055044 (2009).
[26] J. P. D'Incao, H. Suno, and B. D. Esry, Phys. Rev. Lett. **93**, 123201 (2004).
[27] B. Deh *et al.*, Phys. Rev. A **77**, 010701(R) (2008).